Carboniferous isotope stratigraphy

Jitao Chen[1]*, Bo Chen[1] and Isabel P. Montañez[2]

[1]State Key Laboratory of Palaeobiology and Stratigraphy, Nanjing Institute of Geology and Palaeontology and Center for Excellence in Life and Palaeoenvironment, Chinese Academy of Sciences, Nanjing 210008, China

[2]Department of Earth and Planetary Sciences, University of California, Davis, CA 95616, USA

JC, 0000-0001-6898-0963

*Correspondence: jtchen@nigpas.ac.cn

Abstract: We present an updated set of Carboniferous Sr, C and O isotope stratigraphies based on the existing literature, given the importance of chemostratigraphy for stratigraphic correlation in the Carboniferous. The Carboniferous $^{87}Sr/^{86}Sr$ record, constructed using brachiopods and conodonts, exhibits five first-order phases beginning with a rapid decline from a peak value of *c.* 0.70840 at the Devonian–Carboniferous boundary to a trough (0.70776–0.70771) in the Visean followed by a rise to a plateau (*c.* 0.70827) in the upper Bashkirian. A decline to *c.* 0.70804 follows from the lowermost Gzhelian to the close of the Carboniferous. Contemporaneous carbonate $\delta^{13}C$ records exhibit considerable variability between materials analysed and by region, although pronounced excursions (e.g. the mid-Tournaisian positive excursion and the end-Kasimovian negative excursion) are present in most records. Bulk carbonate $\delta^{13}C$ records from South China and Europe, however, are generally consistent with those of brachiopod calcite from North America in terms of both absolute values and trends. Both brachiopod calcite and conodont phosphate $\delta^{18}O$ document large regional variability, confirming that Carboniferous $\delta^{18}O$ records are invalid for precise stratigraphic correlation. Nevertheless, significant positive $\delta^{18}O$ shifts in certain intervals (e.g. mid-Tournaisian and the Mississippian–Pennsylvanian transition) can be used for global correlation.

Supplementary material: Age-updated geochemical data used to build the figures are available at https://doi.org/10.6084/m9.figshare.c.5215784

Isotope stratigraphy can be used for correlation and dating of sedimentary successions (e.g. Montañez *et al.* 1996; Saltzman *et al.* 2000; Chen *et al.* 2018; Garbelli *et al.* 2019), and thus it becomes increasingly important for searching for Global Stratotype Sections and Points (GSSPs). Isotope stratigraphy can also be used to identify stratigraphic completeness and discontinuities (Glumac and Spivak-Birndorf 2002; Chen *et al.* 2011; Z. Wang *et al.* 2020) and spatial variability in biogeochemical cycling of certain isotopes (e.g. Schiffbauer *et al.* 2017; Montañez *et al.* 2018). Therefore, isotope stratigraphy of different elements (e.g. Sr, C and O) is fundamental to integrative stratigraphic studies as well as Earth surface system studies.

Marine fossil taxa such as conodonts, foraminifers, fusulinids and ammonites are commonly used as index fossils for GSSPs of the Carboniferous (Wang *et al.* 2019). These fauna are, however, often facies dependent, thus hampering efforts for effective stratigraphic correlation (e.g. Groves *et al.* 2012; J. Chen *et al.* 2016; Cózar *et al.* 2019). Seawater $\delta^{13}C$ and $^{87}Sr/^{86}Sr$ values recorded in low-temperature marine precipitates are considered to have high potential for stratigraphic correlation and for defining GSSPs (e.g. Saltzman *et al.* 2000, 2014; Chen *et al.* 2018; Garbelli *et al.* 2019). Although there are several existing Carboniferous $^{87}Sr/^{86}Sr$, $\delta^{13}C$ and $\delta^{18}O$ records for Euramerica and South China, these records are characterized by considerable variability in spatial and/or temporal resolution and by the differing types of material analysed (e.g. Mii *et al.* 1999, 2001; Grossman *et al.* 2008; Brand *et al.* 2012; Chen *et al.* 2018; Montañez *et al.* 2018). In this paper, we review the existing Carboniferous Sr, C and O isotope stratigraphies with emphasis on intervals characterized by pronounced isotopic perturbations.

Strontium isotope stratigraphy

Seawater strontium isotopic composition ($^{87}Sr/^{86}Sr$) represents a mixture of two main sources: continent-derived, more radiogenic weathering flux and mantle-derived, less radiogenic volcanic and hydrothermal fluxes (Palmer and Edmond 1989; Davis *et al.* 2003; Allègre *et al.* 2010). Given the long residence time (2–5 myr) of Sr in the oceans relative to the short oceanic mixing time (1–1.5 kyr), at any

From: Lucas, S. G., Schneider, J. W., Wang, X. and Nikolaeva, S. (eds) *The Carboniferous Timescale*. Geological Society, London, Special Publications, **512**,
https://doi.org/10.1144/SP512-2020-72

given time, seawater is thought to be homogeneous with respect to $^{87}Sr/^{86}Sr$. Exceptions, however, may include marginal-marine and estuarine settings with reduced salinities (e.g. Ingram and Sloan 1992; Sharma *et al.* 2007; Bryant *et al.* 2015; Montañez *et al.* 2018). Thus, with this caveat in consideration, seawater $^{87}Sr/^{86}Sr$ has good potential for dating and correlating normal marine successions worldwide, particularly when biostratigraphy is limited and for those stratigraphic intervals characterized by a high rate of change in $^{87}Sr/^{86}Sr$ (e.g. Saltzman *et al.* 2014; Garbelli *et al.* 2019). Uncertainty in $^{87}Sr/^{86}Sr$-based numerical age dating is dependent both on the uncertainty of the $^{87}Sr/^{86}Sr$ calibration curve and on the rate of change in the $^{87}Sr/^{86}Sr$ curve (McArthur *et al.* 2012). For example, a more precise age can be obtained if the uncertainty of the calibration curve is small and the rate of change in $^{87}Sr/^{86}Sr$ is rapid for a given time interval, whereas usage of $^{87}Sr/^{86}Sr$ for age dating and stratigraphic correlation is invalid for intervals with invariable $^{87}Sr/^{86}Sr$ values or with a low rate of change.

Choice of material and diagenesis

For the use of the Sr isotope proxy, however, caution should be taken with respect to the choice of pristine material that can faithfully record the seawater isotopic signature. Given the high susceptibility of carbonates to diagenetic alteration and potential contamination of measured $^{87}Sr/^{86}Sr$ ratios by radiogenic Sr (^{87}Sr) contributed from detrital aluminosilicate phases during acid digestion, bulk carbonates are not the preferential material for constructing palaeoseawater $^{87}Sr/^{86}Sr$ when other diagenesis-resistant biogenic (calcitic and phosphatic) materials exist. Nevertheless, marine-cemented bulk carbonate is the most abundant of the available materials for Sr isotope studies throughout Earth history, and in particular there is no available fossil material in the Precambrian. Thus, carbonates have long been investigated for preservational potential and by acid leaching methods for $^{87}Sr/^{86}Sr$ work. Based on comparison studies of contemporaneous conodont (Saltzman *et al.* 2014) and bulk carbonate (Edwards *et al.* 2015) $^{87}Sr/^{86}Sr$ from the Ordovician in North America, Edwards *et al.* (2015, p. 1275) suggested that bulk carbonates may faithfully record seawater $^{87}Sr/^{86}Sr$ if the samples meet certain screening criteria such as [Sr] >300 ppm and 'minimal thermal alteration, with burial temperatures less than *c.* 150°C'. However, a one-on-one comparison of brachiopods and bulk carbonate $^{87}Sr/^{86}Sr$ suggests that caution should be taken when using cut-off levels of contents and ratios of major and trace elements (e.g. [Sr] and [Mn]) as screening measures (Zaky *et al.* 2019). On the other hand, a sequential carbonate leaching approach was recently developed to isolate the least diagenetically altered carbonate phases from detrital aluminosilicate Sr contamination (Bellefroid *et al.* 2018). Their bulk limestone $^{87}Sr/^{86}Sr$ values, obtained using the sequential leaching method on samples of Mid-Carboniferous Bird Spring carbonates (Arrow Canyon, Nevada, USA), were near identical to the coeval, well-preserved calcite brachiopod $^{87}Sr/^{86}Sr$ values (Bellefroid *et al.* 2018). Lastly, well-preserved, early marine cements are considered to more faithfully record seawater $^{87}Sr/^{86}Sr$ (cf. Zhou *et al.* 2020). Application of early marine cements, however, requires that specific lithofacies (e.g. grainstone and microbialites) occur in the succession of interest and the use of systematic diagenetic screening and micro-drilling techniques. Diagenetic screening typically involves a stepwise process of plane-light petrography, scanning electron microscopy, cathodoluminescence microscopy, and major and trace element evaluation.

Diagenetically screened brachiopods are widely regarded as ideal material for developing $^{87}Sr/^{86}Sr$ as well as for $\delta^{13}C$ and $\delta^{18}O$ records (e.g. Bruckschen *et al.* 1999; Mii *et al.* 1999, 2001; Veizer *et al.* 1999; Grossman *et al.* 2008; Prokoph *et al.* 2008; Brand *et al.* 2009, 2012; Garbelli *et al.* 2019; Zaky *et al.* 2019). However, continuous and high temporal resolution sampling of brachiopods is not possible in many stratigraphic successions, although near continuous sampling of brachiopods at the metre to sub-metre scale is plausible for certain stratigraphic intervals in some carbonate successions (Brand *et al.* 2012; W.-Q. Wang *et al.* 2020). Furthermore, composite isotopic records of brachiopods can be compromised by uncertainties in stratigraphic correlation between sections and regions (Korte and Ullmann 2018).

Conodonts, fossil teeth of nektonic animals, are present in nearly all the Paleozoic marine successions of either shallow- or deeper-water depositional environments, in contrast to benthic brachiopods, which mostly lived on shallow-water shelves. Thus, conodonts have the potential to provide an optimum medium for reconstruction of continuous records of $^{87}Sr/^{86}Sr$. Besides, conodonts are also regarded as being the most resistant to diagenesis based on evaluation of oxygen isotopes (Wenzel *et al.* 2000; Joachimski *et al.* 2009), despite the absence of diagenetic evaluation techniques comparable to those applied to carbonates. Previous studies have shown that conodonts with relatively low to even high colour alteration index (CAI ≤4–5) may preserve pristine seawater geochemistry if properly chemically treated (Ruppel *et al.* 1996; Armstrong *et al.* 2001; John *et al.* 2008; Saltzman *et al.* 2014; Dudás *et al.* 2017; Chen *et al.* 2018; Montañez *et al.* 2018), whereas others show that conodonts can have more radiogenic $^{87}Sr/^{86}Sr$ values than

coeval, well-preserved brachiopods (e.g. Woodard *et al.* 2013; Korte and Ullmann 2018). Conodonts from epicontinental and marginal sea settings may further complicate the construction of seawater Sr isotope records as their $^{87}Sr/^{86}Sr$ values are influenced by sea-specific environmental processes (e.g. riverine influx, long residence times of water masses, evaporation and enhanced stratification) (Montañez *et al.* 2018). Furthermore, conodonts extracted from shales may be problematic given that the high content of easily exchangeable radiogenic Sr in clay minerals can potentially alter the depositional signal (Ebneth *et al.* 1997). In contrast, conodonts extracted from a limestone matrix (with much less radiogenic Sr) generally show similar or lower values compared to coeval brachiopods (e.g. Saltzman *et al.* 2014; Dudás *et al.* 2017; Chen *et al.* 2018), suggesting that conodonts have high potential for $^{87}Sr/^{86}Sr$ studies. Where differences occur in $^{87}Sr/^{86}Sr$ values between presumed coeval conodonts and brachiopods, these differences could be due to uncertainties of stratigraphic correlation and age assignment for individual samples, or they could 'reflect real differences in how conodonts and brachiopods preserve seawater $^{87}Sr/^{86}Sr$' (Saltzman *et al.* 2014, p. 1563).

Carboniferous $^{87}Sr/^{86}Sr$ trend

The existing Carboniferous seawater $^{87}Sr/^{86}Sr$ record, reconstructed from bulk carbonates and brachiopod calcite (Denison *et al.* 1994*b*; Bruckschen *et al.* 1999), remains moderately resolved, limiting its chronostratigraphic and proxy potential. The resolution of the existing record reflects stratigraphic uncertainties and discontinuities, inaccurate correlation among multi-basin records, limited biostratigraphic (temporal) resolution and variable degrees of diagenetic alteration (Cummins and Elderfield 1994; Denison *et al.* 1994*a*; Bruckschen *et al.* 1999; Veizer *et al.* 1999; McArthur *et al.* 2012; Edwards *et al.* 2015). In contrast, the conodont $^{87}Sr/^{86}Sr$ record from a continuous carbonate slope succession (Naqing, South China) (Chen *et al.* 2018) exhibits substantially less variability between contemporaneous samples and generally good consistency with the lower limit of a compilation of brachiopod $^{87}Sr/^{86}Sr$ data (Prokoph *et al.* 2008), except for a significant offset between proxy values in the interval between 330 and 320 Ma (Fig. 1). Given the superiority of both brachiopods and conodonts in recording the seawater $^{87}Sr/^{86}Sr$, the generally overlapping values of the two archives suggest a robust seawater signature.

The Carboniferous $^{87}Sr/^{86}Sr$ trend based on brachiopods and conodonts shows generally five phases through time (Fig. 1) that are broadly consistent with those presented in the *Geological Time Scale 2012*

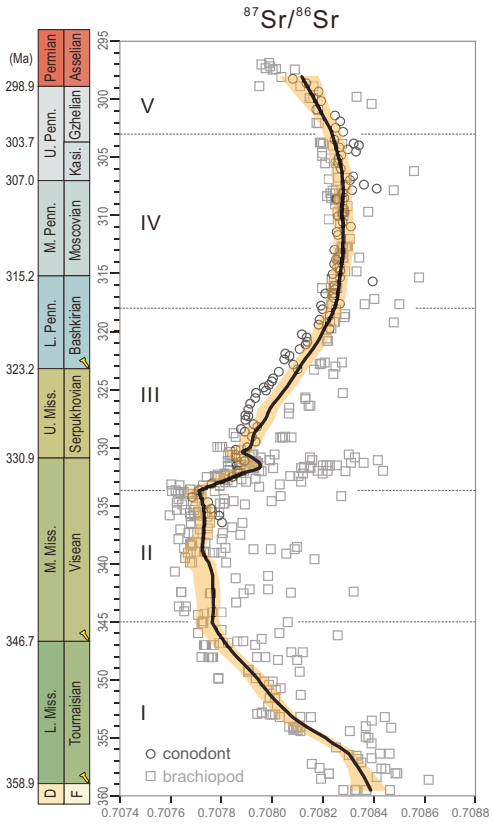

Fig. 1. Carboniferous $^{87}Sr/^{86}Sr$ record constructed using brachiopod dataset (compiled by Prokoph *et al.* 2008) and conodont dataset (Chen *et al.* 2018). The trend line (black) is LOESS regression with 2.5 and 97.5% bootstrapped errors (orange shading). I–V are the five phases of Carboniferous $^{87}Sr/^{86}Sr$ first-order trend discussed in the main text. Ages of all geochemical data are normalized to those of the International Chronostratigraphic Chart (version 2019; http://www.stratigraphy.org). D, Devonian; F, Famennian; Miss, Mississippian; Penn, Pennsylvanian; Kasi, Kasimovian; L, Lower; M, Middle; U, Upper.

(McArthur *et al.* 2012). Differences do exist in absolute values within certain intervals reflecting the use of only biogenic material in the compilation presented here. In the first phase, $^{87}Sr/^{86}Sr$ values at *c.* 360 Ma, proximal to the Devonian–Carboniferous boundary (358.9 Ma), define a peak (*c.* 0.70840) for much of the Devonian and Mississippian periods (McArthur *et al.* 2012). The $^{87}Sr/^{86}Sr$ subsequently declines rapidly (average rate of 0.000043/myr) and near linearly over a *c.* 15 myr period, from peak values down to *c.* 0.70776 at 345 Ma (lowermost Visean). Phase 2 is a trough in $^{87}Sr/^{86}Sr$ values and persists over *c.* 11 myr of the Visean (345–334 Ma), with values decreasing slightly from

0.70776 to 0.70771 in the upper Visean. In the third phase, $^{87}Sr/^{86}Sr$ increases over a *c.* 16 myr period (334–318 Ma) of the Serpukhovian through Bashkirian from *c.* 0.70771 to *c.* 0.70827. There is, however, a short-lived decline from 0.70795 to 0.70788 between 331.7 and 330.4 Ma, close to the Visean–Serpukhovian boundary. To what degree this decline is robust needs to be further tested by high temporal resolution data. A fourth phase is defined by a $^{87}Sr/^{86}Sr$ plateau, which exists over a *c.* 15 myr period (318–303 Ma) of the upper Bashkirian to lowermost Gzhelian, with an average value of *c.* 0.70827. In the final phase, $^{87}Sr/^{86}Sr$ declines through the remainder of the Carboniferous from the plateau to a value of *c.* 0.70814 at the Carboniferous–Permian boundary (298.9 Ma).

Carbon isotope stratigraphy

The carbon isotopic composition of marine carbonates ($\delta^{13}C_{carb}$) has been extensively analysed from successions ranging in age from Precambrian to the present, and is widely used as a tool for stratigraphic correlation, particularly for periods with pronounced positive or negative excursions (Saltzman and Thomas 2012). $\delta^{13}C_{carb}$ values, however, are influenced not only by carbon cycle–climate perturbations, but also by a number of local to regional factors such as mineralogical variability, differences in circulation and residence times of water masses, vital effects, salinity, as well as diagenesis (Algeo *et al.* 1992; Patterson and Walter 1994; Panchuk *et al.* 2005; Swart and Eberli 2005; Batt *et al.* 2007; Swart 2015; Schiffbauer *et al.* 2017; Li *et al.* 2018). Stratigraphic hiatuses may also mask original $\delta^{13}C_{carb}$ stratigraphic features or trends (Glumac and Spivak-Birndorf 2002; Saltzman *et al.* 2004*b*; Chen *et al.* 2011; Roark *et al.* 2017; Maharjan *et al.* 2018*a*; Z. Wang *et al.* 2020). It has been suggested that $\delta^{13}C_{carb}$ excursions of greater magnitude than 1 to 2‰ are those that can be more confidently used for global stratigraphic correlation (Saltzman and Thomas 2012). Furthermore, detailed sedimentological and petrographic study provide the necessary framework in which to evaluate the most robust $\delta^{13}C_{carb}$ data.

Carboniferous $\delta^{13}C_{carb}$ trend

Many studies have evaluated the temporal and spatial variability in $\delta^{13}C_{carb}$ through the Carboniferous, in particular in North America and Russia. These studies are based on brachiopod calcite (e.g. Popp *et al.* 1986; Grossman *et al.* 1993, 2008; Bruckschen *et al.* 1999; Mii *et al.* 1999, 2001; Brand *et al.* 2012) and bulk carbonates (e.g. Saltzman 2002, 2003*a*, *b*, 2005; Batt *et al.* 2007; Dyer *et al.* 2015; Maharjan *et al.* 2018*a*). Over the last decade, new records of Carboniferous $\delta^{13}C_{carb}$ have been developed based on bulk or micro-drilled carbonates from South China (Buggisch *et al.* 2011; Qie *et al.* 2011, 2016; Liu *et al.* 2015, 2017; Yao *et al.* 2015; J. Chen *et al.* 2016; Tian *et al.* 2020). $\delta^{13}C_{carb}$ records from North America, Russia, and South China, however, exhibit moderate to poor agreement (Fig. 2). For example, bulk carbonate $\delta^{13}C$ values of *c.* 3‰ (VPDB, Vienna Pee Dee Belemnite) during the upper Visean to Serpukhovian in South China and Europe (Fig. 2a) are much higher than the coeval $\delta^{13}C$ values in between −2‰ and 2‰ in the Antler foreland basin and Arrow Canyon, North America (Fig. 2b). Such large differences in the coeval $\delta^{13}C_{carb}$ values certainly make carbon isotopes invalid for stratigraphic correlation. In addition, there are large differences in the absolute $\delta^{13}C_{carb}$, trends in regional records, and magnitude of $\delta^{13}C$ changes of records within North America as well as between continents (e.g. Batt *et al.* 2007; Grossman *et al.* 2008). The disparity in carbonate $\delta^{13}C$ for any given interval most likely reflects the aforementioned local to regional variability in palaeoenvironmental and diagenetic conditions and processes that imprint seawater $\delta^{13}C$ signals (Brand *et al.* 2009; Swart 2015). It is also likely that uncertainties in stratigraphic correlation and age assignment between regions account for some of the disparity in datasets. For example, precise stratigraphic correlation between successions in the eastern Palaeo-Tethys Ocean (e.g. South China) and those in the eastern Panthalassic Ocean (e.g. Midcontinent of North America) has long been problematic due to the different conodont biofacies in the Mississippian and palaeogeographical endemism in Pennsylvanian conodonts as a result of closure of the Rheic Ocean (Wang *et al.* 2019). That said, carbonate $\delta^{13}C$ datasets indicate that on the longer term during the Carboniferous, $\delta^{13}C$ rose rapidly from *c.* 0 to 1‰ to *c.* 5 to 7‰ in the earliest Mississippian, remaining high overall (*c.* 3–6‰) through the remainder of the Carboniferous and earliest Permian (i.e. the duration of the Late Paleozoic Ice Age), with superimposed relatively short-lived positive and negative excursions (Fig. 2; Saltzman 2003*b*; Grossman *et al.* 2008; Buggisch *et al.* 2011; Brand *et al.* 2012). The degree to which the shorter-term excursions are robust globally is under evaluated.

Mid-Tournaisian positive $\delta^{13}C_{carb}$ excursion

A pronounced positive excursion in $\delta^{13}C_{carb}$ (with peak values of *c.* 5–7‰) occurs in the middle Tournaisian Stage (roughly during the *Siphonodella isosticha* and *Gnathodus punctatus*/*G. typicus* conodont zones) and has been reported globally, referred to as the TICE (Fig. 2; Mii *et al.* 1999; Saltzman

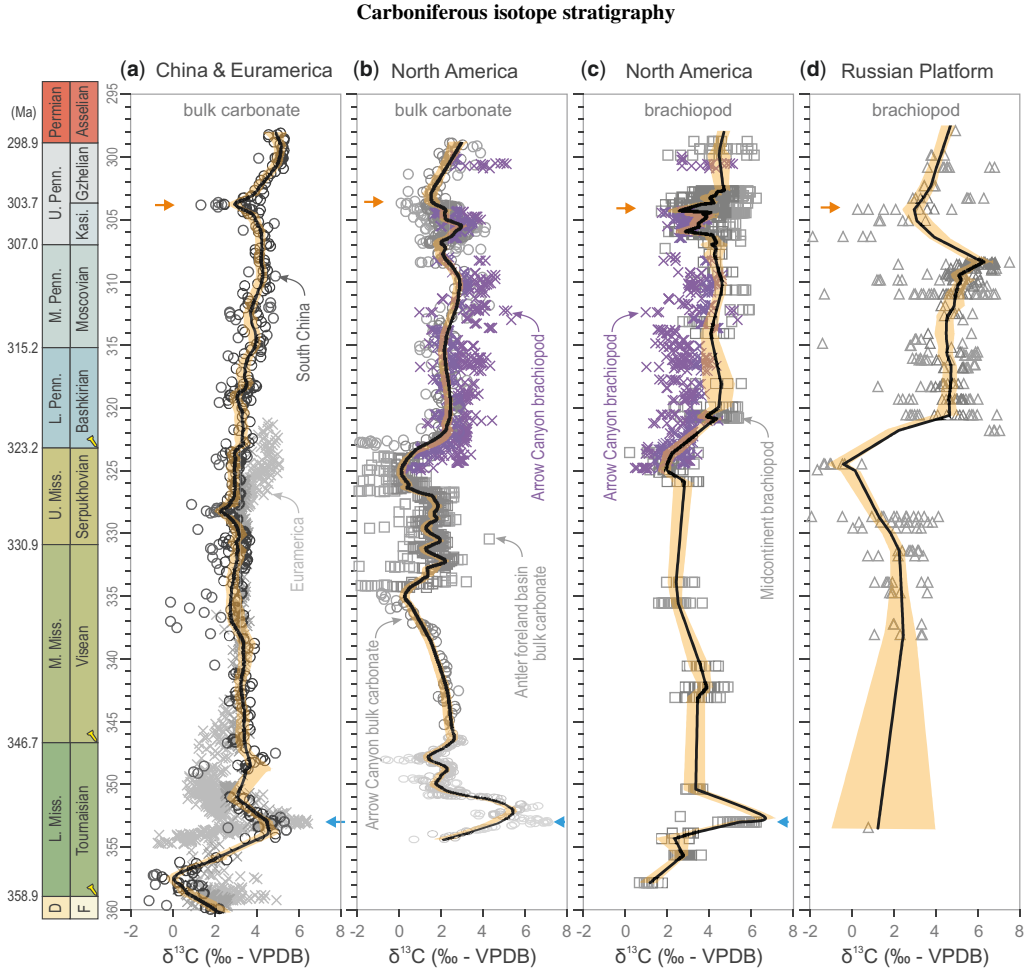

Fig. 2. Carbonate $\delta^{13}C$ exhibiting substantial variability regionally and between materials analysed through the Carboniferous. Trend lines (black) are LOESS regressions with 2.5 and 97.5% bootstrapped errors (orange shading). The mid-Tournaisian positive isotope excursion (TICE; blue arrows) and end-Kasimovian negative isotope excursion (orange arrows) are delineated by all curves except for the Russian Platform. (**a**) Bulk carbonate $\delta^{13}C$ from South China (Buggisch *et al.* 2011; Liu *et al.* 2015; Qie *et al.* 2016) and Euramerica (Buggisch *et al.* 2008). Trend line based on South China data. (**b**) Bulk carbonate $\delta^{13}C$ from Arrow Canyon, Nevada (Saltzman 2003*a*, *b*) and the Antler foreland basin, Idaho (Batt *et al.* 2007) used in *The Geological Time Scale 2012* (Saltzman and Thomas 2012). Trend line based on all bulk carbonate data. Contemporaneous brachiopod $\delta^{13}C$ from Arrow Canyon (Brand *et al.* 2012) for comparison. (**c**) Brachiopod $\delta^{13}C$ from North America: Midcontinent (Grossman *et al.* 2008) and Arrow Canyon (Brand *et al.* 2012). Trend line based on Midcontinent data. (**d**) Brachiopod $\delta^{13}C$ from Russian Platform (Grossman *et al.* 2008). Note, the lighter grey circles in (b) and lighter grey squares in (c) represent a subset $\delta^{13}C$ of Saltzman (2003*a*, *b*) and of Grossman *et al.* (2008) that are compressed (upward by *c.* 4 myr) and shifted (downward by *c.* 2.2 myr), respectively, in order to make the data consistent with the general timing (mid-Tournaisian) of the TICE as in (a). Calibration of ages and abbreviations as in Figure 1.

2002, 2003*a*, 2005; Saltzman *et al.* 2004*a*; Katz *et al.* 2007; Buggisch *et al.* 2008; Yao *et al.* 2015; Qie *et al.* 2016; Maharjan *et al.* 2018*a*). The TICE is contemporaneous with a positive excursion in brachiopod and conodont $\delta^{18}O$, suggesting major cooling and onset of glaciation (Mii *et al.* 1999; Buggisch *et al.* 2008). The TICE is also coincident with a negative excursion in carbonate $\delta^{238}U$ (Cheng *et al.* 2020) and a positive excursion in carbonate-associated sulfate $\delta^{34}S$ and organic matter $\delta^{15}N$. These geochemical records suggest widespread oceanic anoxia associated with enhanced burial of organic C and pyrite, and water-column denitrification (Yao *et al.* 2015; Maharjan *et al.* 2018*a*, *b*; Cheng *et al.* 2020). There are, however, uncertainties with respect to the shape of the $\delta^{13}C$ curve, which

defines either single or double spikes during the TICE (see Maharjan *et al.* 2018*a*). Delineating the spatio-temporal architecture of the TICE is critical to better understanding the origin of this global C perturbation as well as for high-resolution stratigraphic correlation. Better delineation of the TICE architecture requires additional studies on stratigraphically expanded and near-continuous successions, which are also characterized by high-resolution biostratigraphy and/or high-precision U–Pb dating.

Mid-Carboniferous $\delta^{13}C_{carb}$ trend

A positive $\delta^{13}C_{carb}$ shift (by *c.* 1.5–3‰) across the mid-Carboniferous boundary (i.e. Mississippian–Pennsylvanian boundary, MPB) has long been recognized in $\delta^{13}C_{carb}$ records defined using calcite brachiopods (Popp *et al.* 1986; Grossman *et al.* 1993, 2008; Bruckschen *et al.* 1999; Mii *et al.* 1999, 2001), although there are relatively sparse $\delta^{13}C_{carb}$ data or even $\delta^{13}C_{carb}$ stratigraphic gaps associated with the MPB interval. A relatively continuous brachiopod $\delta^{13}C_{carb}$ record from Arrow Canyon exhibits a rapid increase in $\delta^{13}C_{carb}$, from relatively low values (0.5–1‰) to background values (*c.* 3‰), immediately prior to the MPB (Fig. 2b; Brand and Brenckle 2001; Brand *et al.* 2012). Moreover, a high-resolution, composite bulk carbonate $\delta^{13}C$ record from six Euramerican sections indicates a *c.* 2‰ increase through the middle (*c.* 3‰) to upper Serpukhovian (*c.* 5‰), leading up to the MPB (Buggisch *et al.* 2008). In contrast, a high-resolution $\delta^{13}C_{carb}$ time series developed from stratigraphically continuous carbonate slope successions in South China reveals only a *c.* 0.5–1.0‰ increase in $\delta^{13}C_{carb}$ across the MPB (Fig. 2a; Tian *et al.* 2020). Some of the spatial variability in the magnitude of increase in $\delta^{13}C_{carb}$ across the MPB has been attributed to differing intensity of upwelling in the various regions due to differing palaeogeography (Mii *et al.* 2001; Liu *et al.* 2015; Tian *et al.* 2020).

In contrast, Saltzman and Thomas (2012) identified a negative $\delta^{13}C_{carb}$ excursion in the upper Serpukhovian (to the lowermost Bashkirian), recorded in bulk carbonates from western Laurentia (Fig. 2b; Saltzman 2003*b*) and recognized in a bulk $\delta^{13}C_{carb}$ composite record developed using deeper-water carbonate ramp successions in east–central Idaho (Batt *et al.* 2007). Batt *et al.* (2007) argued that their bulk $\delta^{13}C_{carb}$ composite record is not compromised by subaerial exposure or meteoric diagenesis, and their bulk $\delta^{13}C_{carb}$ compares well with a subset of coexisting brachiopod $\delta^{13}C$ values. The latest Serpukhovian and MPB interval in the Arrow Canyon succession, SE Nevada, however, has been shown to include multiple subaerial exposure surfaces (Bishop *et al.* 2009, 2010). On the other hand, low $\delta^{13}C_{carb}$ values in the upper Serpukhovian interval of the Russian Platform brachiopod record (Fig. 2d) may reflect vital effects of the Strophomenata brachiopod, *Gigantoproductus* (e.g. Bruckschen *et al.* 1999; Garbelli *et al.* 2014). Overall, the Russian record shows more scattering and contains a greater proportion of lower $\delta^{13}C_{carb}$ and $\delta^{18}O_{carb}$ values than the brachiopod-based $\delta^{13}C_{carb}$ record from Laurentia (Grossman *et al.* 2008; Brand *et al.* 2012). There are no obvious analogous low values in the bulk carbonate $\delta^{13}C_{carb}$ records from South China (Buggisch *et al.* 2011) and Europe (Buggisch *et al.* 2008; Campion *et al.* 2018), or the Laurentian brachiopod records (Grossman *et al.* 2008). One consideration, however, is that climate simulations for the Carboniferous and early Permian (Montañez and Poulsen 2013; Heavens *et al.* 2015) indicate intensified upwelling on the eastern margin of the Panthalassan Ocean that would provide ^{13}C-depleted seawater into the western regions of palaeotropical Laurentia and could explain the overall lower $\delta^{13}C_{carb}$ values of western Laurentian records (Saltzman 2003*b*; Batt *et al.* 2007) relative to those of the US Midcontinent and Palaeo-Tethyan locales (Buggisch *et al.* 2008; Grossman *et al.* 2008; Tian *et al.* 2020).

End-Kasimovian negative $\delta^{13}C_{carb}$ excursion

A pronounced negative $\delta^{13}C_{carb}$ excursion (by *c.* 2‰) occurs at the end-Kasimovian (*Streptognathodus zethus* or *Idiognathodus naraoensis* conodont zone), recorded in particular in the South China carbonate slope succession (Fig. 2a), although recognizable in the bulk carbonate and brachiopod $\delta^{13}C_{carb}$ records from Laurentia and Russia (Fig. 2). This short-lived negative $\delta^{13}C_{carb}$ excursion is superimposed on an overall rise in $\delta^{13}C_{carb}$ that spans the early Pennsylvanian to early Cisuralian (Buggisch *et al.* 2011). The negative excursion was, however, not formally identified until the recent GSSP search for the base of the Gzhelian in South China (Qi *et al.* 2020). The end-Kasimovian negative $\delta^{13}C_{carb}$ excursion, if proven worldwide, can serve as a reliable tool for chemo-stratigraphic correlation of the Kasimovian–Gzhelian boundary and as a powerful auxiliary stratigraphic marker for the GSSP of the Gzhelian base. The cause and consequences of the carbon perturbation at the end of the Kasimovian are now under study.

Oxygen isotope stratigraphy

Oxygen isotope ratios ($\delta^{18}O$) preserved in marine authigenic carbonates (e.g. early marine cement) and marine carbonate or phosphate fossil skeletons are primarily dependent on temperature and $\delta^{18}O$

of the ambient seawater (Epstein *et al.* 1953). Seawater $\delta^{18}O$ is in turn influenced by changes in continental ice volume and salinity, which is controlled largely by local evaporation/precipitation ratios and surface runoff fluxes to epicontinental seas or oceans. An increase in $\delta^{18}O$ recorded in sedimentary archives can be interpreted as cooling, increased salinity and/or continental ice build-up, whereas a decrease may reflect warming, decreased salinity and/or deglaciation. Rapid changes in seawater $\delta^{18}O$ or temperature can be recorded in $\delta^{18}O$ values of marine authigenic and biogenic carbonates and could possibly be used as chemo-stratigraphic markers for regional and global correlation but solely provided that the seawater signal is not overprinted by subsequent geological processes.

Choice of material and diagenesis

Bulk carbonates are easily altered with respect to their $\delta^{18}O$ by diagenetic fluids (Veizer and Hoefs 1976), and therefore they cannot be used for reconstruction of seawater $\delta^{18}O$, although bulk carbonate $\delta^{18}O$ values are often used to evaluate the potential of diagenetic alteration on $\delta^{13}C_{carb}$ (e.g. Algeo *et al.* 1992; Swart 2015; J. Chen *et al.* 2016; Cui *et al.* 2017). Articulate calcitic brachiopods, which are widely distributed in Phanerozoic strata, are composed of dense microstructures and low-Mg calcite, which are relatively resistant to diagenetic alteration (Compston 1960; Lowenstam 1961; Popp *et al.* 1986; Veizer *et al.* 1986; Brand *et al.* 2012; Garbelli *et al.* 2012; Casella *et al.* 2018). They are thus regarded as the preferential material for reconstruction of seawater $\delta^{18}O$, particularly for the Paleozoic. Nevertheless, a suite of literature shows that kinetic and vital fractionation effects of brachiopods may also influence their oxygen (and carbon) isotopic composition regarding (non) equilibrium with ambient seawater (e.g. Auclair *et al.* 2003; Batt *et al.* 2007; Yamamoto *et al.* 2010; Cusack *et al.* 2012; Garbelli *et al.* 2014; Rollion-Bard *et al.* 2016, 2019), and thus as articulated in the 'Sr isotope stratigraphy' section, careful assessment of preservation is still necessary before interpreting the data as primary seawater signals.

As an alternative, conodont apatite has been increasingly used to reconstruct the Paleozoic seawater $\delta^{18}O$ trends over the last two decades (e.g. Wenzel *et al.* 2000; Joachimski and Buggisch 2002; Joachimski *et al.* 2006; Trotter *et al.* 2008; Sun *et al.* 2012; B. Chen *et al.* 2013, 2016; Bartlett *et al.* 2018; Jin *et al.* 2018; Montañez *et al.* 2018). Biogenetic phosphates are thought to be more resistant to diagenetic alteration than biogenetic carbonates (e.g. Wenzel *et al.* 2000; Joachimski *et al.* 2009), which may be attributed to extremely slow rates of oxygen isotope exchange between phosphates and water at ambient temperatures via inorganic reactions (Blake *et al.* 1997). Diagenetic alteration is, however, still possible when the oxygen exchange is mediated by enzymes (Zazzo *et al.* 2004) or at high temperatures (Pucéat *et al.* 2004). Unfortunately, diagenetic evaluation methods for calcitic shells are found to have limited application to conodont apatite (Buggisch *et al.* 2008). Furthermore, conodonts are assumed to be nektonic animals that could have thrived in both deep- and shallow-water settings (Orchard 1996; Lai *et al.* 2001), in contrast to brachiopods that normally lived in benthic habitats of relative shallow-water settings. Conodonts, unlike benthic brachiopods, could also easily swim to their preferred settings, and thus a given taxa could record invariant seawater-temperature signals, although secular changes in seawater temperature should be discernible as long as glacio-eustatic and/or salinity changes were minimal (cf. W.-Q. Wang *et al.* 2020). Therefore, different habitats of conodonts need be considered when using their $\delta^{18}O$ records to reconstruct seawater temperatures or seawater $\delta^{18}O$ as a proxy of the magnitude of glacio-eustasy (Hermann *et al.* 2015).

Carboniferous $\delta^{18}O$ trends

The Carboniferous witnessed dramatic glaciation in the southern hemisphere (Gondwana) (Isbell *et al.* 2003, 2012; Fielding *et al.* 2008; Montañez and Poulsen 2013; Griffis *et al.* 2018, 2019), with large magnitude $\delta^{18}O$ shifts interpreted to record major climatic cooling and/or ice volume changes (e.g. Popp *et al.* 1986; Grossman *et al.* 1993; Mii *et al.* 1999, 2001; Joachimski *et al.* 2006; Buggisch *et al.* 2008; B. Chen *et al.* 2016). The most complete Carboniferous $\delta^{18}O$ records are composite and built primarily on brachiopods from the North American Midcontinent and the Russian Platform (Fig. 3a and b; Mii *et al.* 1999, 2001; Grossman *et al.* 2008), whereas continuous conodont apatite $\delta^{18}O$ records are constructed mainly based on data from South China and Europe (Fig. 3c; Buggisch *et al.* 2008; B. Chen *et al.* 2016; Montañez *et al.* 2018). It is notable that the compilation of Carboniferous conodont $\delta^{18}O$ records exhibits large regional differences (Fig. 3c), with data from a more open-water setting (South China) yielding overall higher and less variable values compared to those from epicontinental seas (US Midcontent and Donets Basin, Ukraine). These differences may be attributed to spatial variability in seawater salinity and thus seawater $\delta^{18}O$ gradients in epicontinental seas relative to the more open waters of South China (Rosenau *et al.* 2014; Joachimski and Lambert 2015; Montañez *et al.* 2018). However, differential diagenetic overprint on conodonts from different basins cannot be excluded, although systematic diagenetic screening

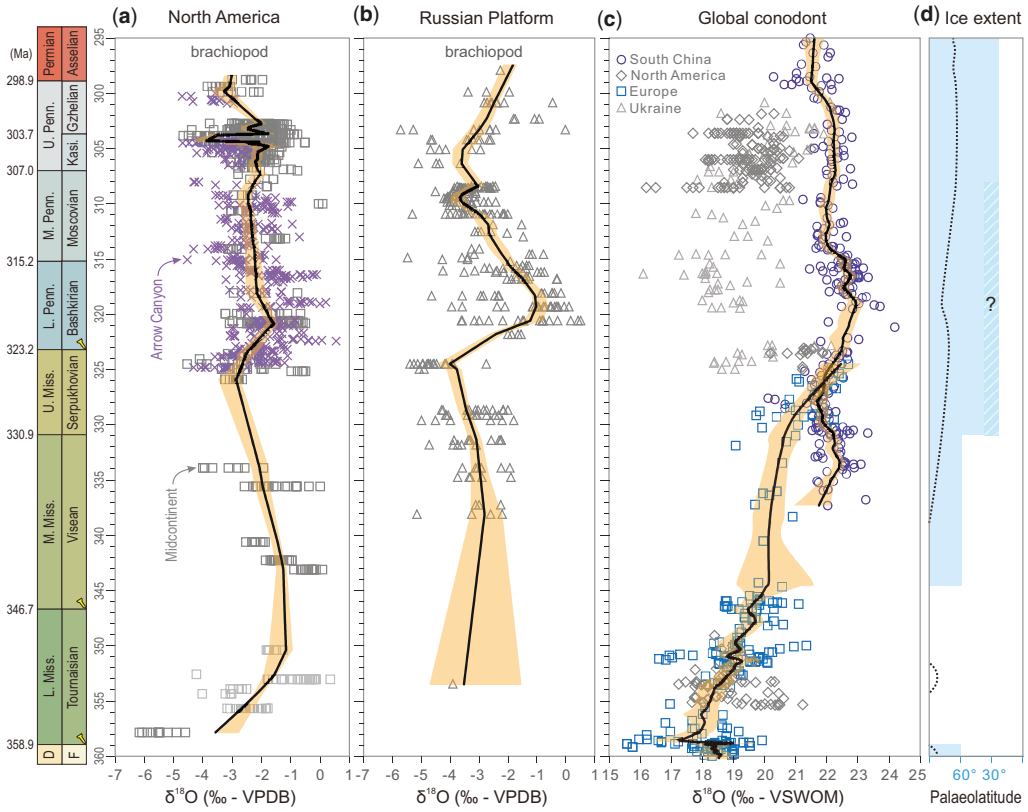

Fig. 3. Carbonate and phosphate $\delta^{18}O$ trends through the Carboniferous. Trend lines (black) are LOESS regressions with 2.5 and 97.5% bootstrapped errors (orange shading). (**a**) Brachiopod $\delta^{18}O$ from the Midcontinent (Grossman *et al.* 2008) and Arrow Canyon, Nevada (Brand *et al.* 2012). Trend lines based on Midcontinent data. Note, the lighter grey squares represent a subset $\delta^{18}O$ of Grossman *et al.* (2008) that are shifted (downward by *c.* 2.2 myr) based on correlation by the TICE. (**b**) Brachiopod $\delta^{18}O$ from the Russian Platform (Grossman *et al.* 2008). (**c**) Conodont $\delta^{18}O$ from South China (B. Chen *et al.* 2016), North America (Joachimski *et al.* 2006; Wallace and Elrick 2014; Joachimski and Lambert 2015), Europe (Buggisch *et al.* 2008) and Ukraine (Montañez *et al.* 2018) exhibiting large regional variations in $\delta^{18}O$. Two sets of trend lines are based on data from B. Chen *et al.* (2016) and Buggisch *et al.* (2008), respectively. (**d**) Qualitative estimate for spread of glacial ice (dot line; Crowell 1999) and palaeolatitude of ice extent (blue shade; Frakes and Francis 1988). Calibration of ages and abbreviations as in Figure 1.

is not plausible. In the overlapping interval (upper Visean to lower Serpukhovian), the South China and Europe conodont $\delta^{18}O$ records show a *c.* 2‰ offset, which may be a consequence of the regional differences in seawater salinity and regional climate. Nevertheless, all of the $\delta^{18}O$ records, including the Donets epicontinental sea record (Fig. 3c), delineate two major, widely recognized trends: (1) a positive shift in the middle Tournaisian (358.9–350 Ma) and (2) a positive shift across the MPB (*c.* 325–320 Ma).

Mid-Tournaisian positive $\delta^{18}O$ shift

Mii *et al.* (1999) found a major increase in $\delta^{18}O$ from −5‰ to −2‰ (VPDB) in the middle Tournaisian (358.9–350 Ma) based on brachiopods from North America (Fig. 3a), which was interpreted as evidence of climate cooling and ice build-up (Mii *et al.* 1999). This shift, however, was not confirmed by the $\delta^{18}O$ record from the Russian Platform due to lack of time-equivalent brachiopods (Fig. 3b). Grossman *et al.* (2008) considered that the positive $\delta^{18}O$ shift may reflect an increase in regional seawater $\delta^{18}O$ as a result of excessive evaporation in North American epicontinental seas. A similar increase (by *c.* 2‰, Vienna Standard Mean Ocean Water (VSMOW)) in conodont apatite $\delta^{18}O$ was subsequently found in low-latitude Euramerican sections (Fig. 3c; Buggisch *et al.* 2008), suggesting that the positive $\delta^{18}O$ shift is a global phenomenon. This $\delta^{18}O$ increase is coincident with a significant $\delta^{13}C$ positive excursion (TICE). The concurrent $\delta^{13}C$ and $\delta^{18}O$ excursions

are in good agreement with the widely held interpretation that increased organic carbon burial (Saltzman 2003*b*; Saltzman *et al.* 2004*a*) resulted in lowered atmospheric pCO_2 and triggered climate cooling (Mii *et al.* 1999; Buggisch *et al.* 2008).

Mid-Carboniferous positive $\delta^{18}O$ shift

A pronounced increase in brachiopod $\delta^{18}O$ has long been observed across the MPB in Euramerica (Fig. 3a and b; Mii *et al.* 1999, 2001; Grossman *et al.* 2008; Brand *et al.* 2012), which is also recorded in conodont apatite $\delta^{18}O$ from several Euramerican basins (Buggisch *et al.* 2008; Montañez *et al.* 2018) and from a carbonate slope succession from South China (B. Chen *et al.* 2016) (Fig. 3c), indicating that it is of global significance. The $\delta^{18}O$ increase coincides with a major glacio-eustatic fall recorded in low-latitude successions (Eros *et al.* 2012*a*, *b*; Tian *et al.* 2020) and the occurrence of widespread glacial depositional records in southern Gondwana (Gulbranson *et al.* 2010; Isbell *et al.* 2012), suggesting significant climate cooling combined with ice build-up across the MPB interval (Mii *et al.* 1999; Buggisch *et al.* 2008; Fielding *et al.* 2008; B. Chen *et al.* 2016). It has been hypothesized that MPB cooling was caused by increased burial of organic carbon, implied by previously reported large increases (by *c.* 3.0‰) in $\delta^{13}C_{carb}$ (e.g. Popp *et al.* 1986; Mii *et al.* 2001). However, there is no significant increase in $\delta^{13}C$ of bulk carbonates across the MPB from the Great Basin, USA (rather a negative excursion; Fig. 2b) (Saltzman 2003*b*) or from the Qian-Gui Bain, South China (Tian *et al.* 2020). Instead, a significant rise in $^{87}Sr/^{86}Sr$ (Chen *et al.* 2018) slightly predates the rise in $\delta^{18}O$ (B. Chen *et al.* 2016), suggesting that climate cooling might have been triggered mainly by enhanced silicate weathering driven by the influence of the Hercynian Orogeny on erosion rates and precipitation and surface hydrology (Goddéris *et al.* 2017; Richey *et al.* 2020), rather than increased burial of organic carbon (Tian *et al.* 2020).

Concluding remarks

The Carboniferous saw the main pulses of Earth's penultimate icehouse, which was a time of low atmospheric pCO_2, extensive glaciation, major tectonic reconfiguration, radiation of palaeotropical rainforests, and a series of climatic and biotic perturbations. Carboniferous isotope geochemistry and stratigraphy play an important role in better understanding these events and their impacts on palaeoclimate and palaeoceanography as well as on biosphere. However, there are a number of environmental, vital and diagenetic factors that can imprint global marine isotopic signatures, which are archived in low-temperature precipitates (carbonates and phosphates). Prior to stratigraphic correlation or chronostratigraphic dating of successions worldwide using Sr, C and O isotopes, diagenetic screening of pristine material as well as evaluation of overall depositional settings (e.g. seawater circulation and salinity, palaeobathymetry, and depositional and regional climate processes) should be carefully considered. In most cases, diagenesis increases the $^{87}Sr/^{86}Sr$ ratios of low-temperature precipitates given the presence of easily exchangeable radiogenic Sr in sediment, although shifts to less radiogenic values has been documented. We take the LOESS regression line of brachiopod and conodont $^{87}Sr/^{86}Sr$ data as the smoothed $^{87}Sr/^{86}Sr$ curve, but there is a big cloud of more radiogenic data (above the regression line), especially for the interval between the upper Tournaisian to the upper Visean. Caution should be taken particularly when dealing with a small dataset for stratigraphic correlation. Large regional differences in carbonate $\delta^{13}C$ and $\delta^{18}O$ and phosphate $\delta^{18}O$ datasets hamper using absolute values for stratigraphic correlation or dating. That said, the existence of multiple, widely recorded and significant excursions in Sr, C and O isotope compositions (e.g. the mid-Tournaisian and end-Kasimovian) offer high potential for stratigraphic correlation. Further refinement of these Sr, C and O isotope records through the Carboniferous, in particular if integrated with efforts to radioisotopically date or astrochronologically constrain the successions, can provide not only robust tools for stratigraphic correlation but also fundamental datasets for biogeochemical modelling of Earth's penultimate icehouse.

Acknowledgements We thank S. Lucas and J.W. Schneider for the invitation to prepare the paper and for their editorial handling. We also appreciate the helpful comments from C. Garbelli and an anonymous reviewer, which greatly improved the manuscript. We thank M. R. Saltzman, W. Qie, L. Yao and C. Liu for sharing their published or compiled Carboniferous $\delta^{13}C$ data. Discussions with K. Hu on Carboniferous conodont biostratigraphy were helpful.

Author contributions **JC**: conceptualization (lead), writing – original draft (lead), writing – review & editing (lead); **BC**: writing – original draft (supporting); **IPM**: writing – review & editing (supporting).

Funding This research was supported by the Strategic Priority Research Program of the Chinese Academy of Sciences grant XDB26000000 (to JC), the National Natural Science Foundation of China grants 42072035, 41672101 and 41630101 (to JC), and the US National Science Foundation grants EAR1338281 and EAR1554897 (to IPM).

Data availability The datasets generated during and/or analysed during the current study are available at https://doi.org/10.6084/m9.figshare.c.5215784, or upon request from the corresponding author.

References

Algeo, T.J., Wilkinson, B.H. and Lohmann, K.C. 1992. Meteoric-burial diagenesis of middle Pennsylvanian limestones in the Orogrande Basin, New Mexico: water/rock interactions and basin geothermics. *Journal of Sedimentary Petrology*, **62**, 652–670.

Allègre, C.J., Louvat, P., Gaillardet, J., Meynadier, L., Rad, S. and Capmas, F. 2010. The fundamental role of island arc weathering in the oceanic Sr isotope budget. *Earth and Planetary Science Letters*, **292**, 51–56, https://doi.org/10.1016/j.epsl.2010.01.019

Armstrong, H.A., Pearson, D.G. and Griselin, M. 2001. Thermal effects on rare earth element and strontium isotope chemistry in single conodont elements. *Geochimica et Cosmochimica Acta*, **65**, 435–441, https://doi.org/10.1016/S0016-7037(00)00548-2

Auclair, A.-C., Joachimski, M.M. and Lécuyer, C. 2003. Deciphering kinetic, metabolic and environmental controls on stable isotope fractionations between seawater and the shell of *Terebratalia transversa* (Brachiopoda). *Chemical Geology*, **202**, 59–78, https://doi.org/10.1016/s0009-2541(03)00233-x

Bartlett, R., Elrick, M., Wheeley, J.R., Polyak, V., Desrochers, A. and Asmerom, Y. 2018. Abrupt global-ocean anoxia during the Late Ordovician-early Silurian detected using uranium isotopes of marine carbonates. *Proceedings of the National Academy of Sciences*, **115**, 5896–5901, https://doi.org/10.1073/pnas.1802438115

Batt, L.S., Montañez, I.P., Isaacson, P., Pope, M.C., Butts, S.H. and Abplanalp, J. 2007. Multi-carbonate component reconstruction of mid-Carboniferous (Chesterian) seawater $\delta^{13}C$. *Palaeogeography, Palaeoclimatology, Palaeoecology*, **256**, 298–318, https://doi.org/10.1016/j.palaeo.2007.02.049

Bellefroid, E.J., Planavsky, N.J., Miller, N.R., Brand, U. and Wang, C. 2018. Case studies on the utility of sequential carbonate leaching for radiogenic strontium isotope analysis. *Chemical Geology*, **497**, 88–99, https://doi.org/10.1016/j.chemgeo.2018.08.025

Bishop, J.W., Montañez, I.P., Gulbranson, E.L. and Brenckle, P.L. 2009. The onset of mid-Carboniferous glacio-eustasy: sedimentologic and diagenetic constraints, Arrow Canyon, Nevada. *Palaeogeography, Palaeoclimatology, Palaeoecology*, **276**, 217–243, https://doi.org/10.1016/j.palaeo.2009.02.019

Bishop, J.W., Montanez, I.P. and Osleger, D.A. 2010. Dynamic Carboniferous climate change, Arrow Canyon, Nevada. *Geosphere*, **6**, 1–34, https://doi.org/10.1130/ges00192.1

Blake, R.E., O'Neil, J.R. and Garcia, G.A. 1997. Oxygen isotope systematics of biologically mediated reactions of phosphate: I. Microbial degradation of organophosphorus compounds. *Geochimica et Cosmochimica Acta*, **61**, 4411–4422, https://doi.org/10.1016/S0016-7037(97)00272-X

Brand, U. and Brenckle, P. 2001. Chemostratigraphy of the Mid-Carboniferous boundary Global Stratotype Section and Point (GSSP), Bird Spring Formation, Arrow Canyon, Nevada, USA. *Palaeogeography Palaeoclimatology Palaeoecology*, **165**, 321–347, https://doi.org/10.1016/S0031-0182(00)00169-3

Brand, U., Tazawa, J.I., Sano, H., Azmy, K. and Lee, X. 2009. Is mid-late Paleozoic ocean-water chemistry coupled with epeiric seawater isotope records? *Geology*, **37**, 823–826, https://doi.org/10.1130/g30038a.1

Brand, U., Jiang, G., Azmy, K., Bishop, J. and Montañez, I.P. 2012. Diagenetic evaluation of a Pennsylvanian carbonate succession (Bird Spring Formation, Arrow Canyon, Nevada, USA) – 1: Brachiopod and whole rock comparison. *Chemical Geology*, **308–309**, 26–39, https://doi.org/10.1016/j.chemgeo.2012.03.017

Bruckschen, P., Oesmann, S. and Veizer, J. 1999. Isotope stratigraphy of the European Carboniferous: proxy signals for ocean chemistry, climate and tectonics. *Chemical Geology*, **161**, 127–163, https://doi.org/10.1016/S0009-2541(99)00084-4

Bryant, J.D., Jones, D.S. and Mueller, P.A. 2015. Influence of freshwater flux on $^{87}Sr/^{86}Sr$ chronostratigraphy in marginal marine environments and dating of vertebrate and invertebrate faunas. *Journal of Paleontology*, **69**, 1–6, https://doi.org/10.1017/s002233600002686x

Buggisch, W., Joachimski, M.M., Sevastopulo, G. and Morrow, J.R. 2008. Mississippian $\delta^{13}C_{carb}$ and conodont apatite $\delta^{18}O$ records – their relation to the Late Palaeozoic Glaciation. *Palaeogeography, Palaeoclimatology, Palaeoecology*, **268**, 273–292, https://doi.org/10.1016/j.palaeo.2008.03.043

Buggisch, W., Wang, X., Alekseev, A.S. and Joachimski, M.M. 2011. Carboniferous–Permian carbon isotope stratigraphy of successions from China (Yangtze platform), USA (Kansas) and Russia (Moscow Basin and Urals). *Palaeogeography, Palaeoclimatology, Palaeoecology*, **301**, 18–38, https://doi.org/10.1016/j.palaeo.2010.12.015

Campion, A., Maloof, A. *et al*. 2018. Constraining the timing and amplitude of early Serpukhovian glacioeustasy with a continuous carbonate record in Northern Spain. *Geochemistry, Geophysics, Geosystems*, **19**, 2647–2660, https://doi.org/10.1029/2017gc007369

Casella, L.A., Griesshaber, E. *et al*. 2018. Micro- and nanostructures reflect the degree of diagenetic alteration in modern and fossil brachiopod shell calcite: a multi-analytical screening approach (CL, FE-SEM, AFM, EBSD). *Palaeogeography, Palaeoclimatology, Palaeoecology*, **502**, 13–30, https://doi.org/10.1016/j.palaeo.2018.03.011

Chen, B., Joachimski, M.M. *et al*. 2013. Permian ice volume and palaeoclimate history: oxygen isotope proxies revisited. *Gondwana Research*, **24**, 77–89, https://doi.org/10.1016/j.gr.2012.07.007

Chen, B., Joachimski, M.M., Wang, X.-D., Shen, S.-Z., Qi, Y.-P. and Qie, W.-K. 2016. Ice volume and paleoclimate history of the Late Paleozoic Ice Age from conodont apatite oxygen isotopes from Naqing (Guizhou, China). *Palaeogeography, Palaeoclimatology, Palaeoecology*, **448**, 151–161, https://doi.org/10.1016/j.palaeo.2016.01.002

Chen, J., Chough, S.K., Han, Z. and Lee, J.-H. 2011. An extensive erosion surface of a strongly deformed

limestone bed in the Gushan and Chaomidian formations (late Middle Cambrian to Furongian), Shandong Province, China: sequence–stratigraphic implications. *Sedimentary Geology*, **233**, 129–149, https://doi.org/10.1016/j.sedgeo.2010.11.002

Chen, J., Montañez, I.P., Qi, Y., Wang, X., Wang, Q. and Lin, W. 2016. Coupled sedimentary and $\delta^{13}C$ records of late Mississippian platform-to-slope successions from South China: Insight into $\delta^{13}C$ chemostratigraphy. *Palaeogeography, Palaeoclimatology, Palaeoecology*, **448**, 162–178, https://doi.org/10.1016/j.palaeo.2015.10.051

Chen, J., Montañez, I.P., Qi, Y., Shen, S. and Wang, X. 2018. Strontium and carbon isotopic evidence for decoupling of pCO_2 from continental weathering at the apex of the late Paleozoic glaciation. *Geology*, **46**, 395–398, https://doi.org/10.1130/g40093.1

Cheng, K., Elrick, M. and Romaniello, S.J. 2020. Early Mississippian ocean anoxia triggered organic carbon burial and late Paleozoic cooling: evidence from uranium isotopes recorded in marine limestone. *Geology*, **48**, 363–367, https://doi.org/10.1130/g46950.1

Compston, W. 1960. The carbon isotopic composition of certain marine invertebrates and coals from the Australian Permian. *Geochimica et Cosmochimica Acta*, **18**, 1–22, https://doi.org/10.1016/0016-7037(60)90013-2

Cózar, P., Izart, A., Somerville, I.D., Aretz, M., Coronado, I., Vachard, D. and Webster, J. 2019. Environmental controls on the development of Mississippian microbial carbonate mounds and platform limestones in southern Montagne Noire (France). *Sedimentology*, **66**, 2392–2424, https://doi.org/10.1111/sed.12594

Crowell, J.C. 1999. Pre-Mesozoic ice ages: their bearing on understanding the climate system. *Geological Society of America Memoir*, **192**, https://doi.org/10.1130/0-8137-1192-4.1

Cui, H., Kaufman, A.J., Xiao, S., Zhou, C. and Liu, X.-M. 2017. Was the Ediacaran Shuram Excursion a globally synchronized early diagenetic event? Insights from methane-derived authigenic carbonates in the uppermost Doushantuo Formation, South China. *Chemical Geology*, **450**, 59–80, https://doi.org/10.1016/j.chemgeo.2016.12.010

Cummins, D.I. and Elderfield, H. 1994. The strontium isotopic composition of Brigantian (late Dinantian) seawater. *Chemical Geology*, **118**, 255–270, https://doi.org/10.1016/0009-2541(94)90180-5

Cusack, M., Huerta, A.P. and EIMF. 2012. Brachiopods recording seawater temperature – A matter of class or maturation? *Chemical Geology*, **334**, 139–143, https://doi.org/10.1016/j.chemgeo.2012.10.021

Davis, A.C., Bickle, M.J. and Teagle, D.A.H. 2003. Imbalance in the oceanic strontium budget. *Earth and Planetary Science Letters*, **211**, 173–187, https://doi.org/10.1016/S0012-821X(03)00191-2

Denison, R.E., Koepnick, R.B., Fletcher, C.H., Howell, M.W. and Callaway, W.S. 1994*a*. Criteria for the retention of original seawater $^{87}Sr/^{86}Sr$ in ancient shelf limestones. *Chemical Geology*, **112**, 131–143, https://doi.org/10.1016/0009-2541(94)90110-4

Denison, R.E., Koepnick, R.B., Burke, W.H., Hetherington, E.A. and Fletcher, C.H. 1994*b*. Construction of the Mississippian, Pennsylvanian and Permian seawater $^{87}Sr/^{86}Sr$ curve. *Chemical Geology*, **112**, 145–167, https://doi.org/10.1016/0009-2541(94)90111-2

Dudás, F.Ö., Yuan, D.-X., Shen, S.-Z. and Bowring, S.A. 2017. A conodont-based revision of the $^{87}Sr/^{86}Sr$ seawater curve across the Permian-Triassic boundary. *Palaeogeography, Palaeoclimatology, Palaeoecology*, **470**, 40–53, https://doi.org/10.1016/j.palaeo.2017.01.007

Dyer, B., Maloof, A.C. and Higgins, J.A. 2015. Glacioeustasy, meteoric diagenesis, and the carbon cycle during the Middle Carboniferous. *Geochemistry, Geophysics, Geosystems*, **16**, 3383–3399, https://doi.org/10.1002/2015gc006002

Ebneth, S., Diener, A., Buhl, D. and Veizer, J. 1997. Strontium isotope systematics of conodonts: Middle Devonian, Eifel Mountains, Germany. *Palaeogeography Palaeoclimatology Palaeoecology*, **132**, 79–96, https://doi.org/10.1016/S0031-0182(97)00057-6

Edwards, C.T., Saltzman, M.R. *et al*. 2015. Strontium isotope ($^{87}Sr/^{86}Sr$) stratigraphy of Ordovician bulk carbonate: Implications for preservation of primary seawater values. *Geological Society of America Bulletin*, **127**, 1275–1289, https://doi.org/10.1130/b31149.1

Epstein, S., Buchsbaum, R., Lowenstam, H.A. and Urey, H.C. 1953. Revised carbonate–water isotopic temperature scale. *Geological Society of America Bulletin*, **64**, 1315–1326, https://doi.org/10.1130/0016-7606(1953)64[1315:Rcits]2.0.Co;2

Eros, J.M., Montañez, I.P., Osleger, D.A., Davydov, V.I., Nemyrovska, T.I., Poletaev, V.I. and Zhykalyak, M.V. 2012*a*. Sequence stratigraphy and onlap history of the Donets Basin, Ukraine: insight into Carboniferous icehouse dynamics. *Palaeogeography, Palaeoclimatology, Palaeoecology*, **313–314**, 1–25, https://doi.org/10.1016/j.palaeo.2011.08.019

Eros, J.M., Montañez, I.P., Davydov, V.I., Osleger, D.A., Nemyrovska, T.I., Poletaev, V.I. and Zhykalyak, M.V. 2012*b*. Reply to the comment on 'Sequence stratigraphy and onlap history of the Donets Basin, Ukraine: insight into Carboniferous icehouse dynamics'. *Palaeogeography, Palaeoclimatology, Palaeoecology*, **363–364**, 187–191, https://doi.org/10.1016/j.palaeo.2012.09.013

Fielding, C.R., Frank, T.D., Birgenheier, L.P., Rygel, M.C. and Jones, A.T. 2008. Stratigraphic imprint of the Late Paleozoic Ice Age in eastern Australia: a record of alternating glacial and nonglacial climate regime. *Journal of the Geological Society, London*, **165**, 129–140, https://doi.org/10.1144/0016-76492007-036

Frakes, L.A. and Francis, J.E. 1988. A guide to Phanerozoic cold polar climates from high-latitude ice-rafting in the Cretaceous. *Nature*, **333**, 547–49.

Garbelli, C., Angiolini, L., Jadoul, F. and Brand, U. 2012. Micromorphology and differential preservation of Upper Permian brachiopod low-Mg calcite. *Chemical Geology*, **298–299**, 1–10, https://doi.org/10.1016/j.chemgeo.2011.12.019

Garbelli, C., Angiolini, L., Brand, U. and Jadoul, F. 2014. Brachiopod fabric, classes and biogeochemistry: Implications for the reconstruction and interpretation of seawater carbon-isotope curves and records. *Chemical Geology*, **371**, 60–67, https://doi.org/10.1016/j.chemgeo.2014.01.022

Garbelli, C., Shen, S.Z. *et al*. 2019. Timing of Early and Middle Permian deglaciation of the southern hemisphere: Brachiopod-based $^{87}Sr/^{86}Sr$ calibration. *Earth and Planetary Science Letters*, **516**, 122–135, https://doi.org/10.1016/j.epsl.2019.03.039

Glumac, B. and Spivak-Birndorf, M.L. 2002. Stable isotopes of carbon as an invaluable stratigraphic tool: an example from the Cambrian of the northern Appalachians, USA. *Geology*, **30**, 563–566, https://doi.org/10.1130/0091-7613(2002)030<0563:SIOCAA>2.0.CO;2

Goddéris, Y., Donnadieu, Y., Carretier, S., Aretz, M., Dera, G., Macouin, M. and Regard, V. 2017. Onset and ending of the late Palaeozoic ice age triggered by tectonically paced rock weathering. *Nature Geoscience*, **10**, 382–386, https://doi.org/10.1038/ngeo2931

Griffis, N.P., Mundil, R. *et al*. 2018. A new stratigraphic framework built on U–Pb single-zircon TIMS ages and implications for the timing of the penultimate icehouse (Paraná Basin, Brazil). *Geological Society of America Bulletin*, **130**, 848–858, https://doi.org/10.1130/b31775.1

Griffis, N.P., Montañez, I.P. *et al*. 2019. Coupled stratigraphic and U-Pb zircon age constraints on the late Paleozoic icehouse-to-greenhouse turnover in south-central Gondwana. *Geology*, **47**, 1146–1150, https://doi.org/10.1130/g46740.1

Grossman, E.L., Mii, H.-S. and Yancey, T.E. 1993. Stable isotopes in Late Pennsylvanian brachiopods from the United States: implications for Carboniferous paleoceanography. *Geological Society of America Bulletin*, **105**, 1284–1296, https://doi.org/10.1130/0016-7606(1993)105<1284:SIILPB>2.3.CO;2

Grossman, E.L., Yancey, T.E., Jones, T.E., Bruckschen, P., Chuvashov, B., Mazzullo, S.J. and Mii, H.-S. 2008. Glaciation, aridification, and carbon sequestration in the Permo-Carboniferous: the isotopic record from low latitudes. *Palaeogeography, Palaeoclimatology, Palaeoecology*, **268**, 222–233, https://doi.org/10.1016/j.palaeo.2008.03.053

Groves, J.R., Yue, W., Yuping, Q., Richards, B.C., Ueno, K. and Xiangdong, W. 2012. Foraminiferal Biostratigraphy of the Visean–Serpukhovian (Mississippian) Boundary Interval at Slope and Platform Sections in Southern Guizhou (South China). *Journal of Paleontology*, **86**, 753–774, https://doi.org/10.1666/11-111.1

Gulbranson, E.L., Montanez, I.P., Schmitz, M.D., Limarino, C.O., Isbell, J.L., Marenssi, S.A. and Crowley, J.L. 2010. High-precision U–Pb calibration of Carboniferous glaciation and climate history, Paganzo Group, NW Argentina. *Geological Society of America Bulletin*, **122**, 1480–1498, https://doi.org/10.1130/b30025.1

Heavens, N.G., Mahowald, N.M., Soreghan, G.S., Soreghan, M.J. and Shields, C.A. 2015. A model-based evaluation of tropical climate in Pangaea during the late Palaeozoic icehouse. *Palaeogeography, Palaeoclimatology, Palaeoecology*, **425**, 109–127, https://doi.org/10.1016/j.palaeo.2015.02.024

Hermann, A.D., Barrick, J.E. and Algeo, T.J. 2015. The relationship of conodont biofacies to spatially variable water mass properties in the Late Pennsylvanian Midcontinent Sea. *Paleoceanography*, **30**, 269–283, https://doi.org/10.1002/2014PA002725

Ingram, B.L. and Sloan, D. 1992. Strontium isotopic composition of estuarine sediments as paleosabity-paleoclirnate indicator. *Science*, **255**, 68–72, https://doi.org/10.1126/science.255.5040.68

Isbell, J.L., Lenaker, P.A., Askin, R.A., Miller, M.F. and Babcock, L.E. 2003. Reevaluation of the timing and extent of late Paleozoic glaciation in Gondwana: role of the Transantarctic Mountains. *Geology*, **31**, 977–980, https://doi.org/10.1130/G19810.1

Isbell, J.L., Henry, L.C. *et al*. 2012. Glacial paradoxes during the late Paleozoic ice age: evaluating the equilibrium line altitude as a control on glaciation. *Gondwana Research*, **22**, 1–19, https://doi.org/10.1016/j.gr.2011.11.005

Jin, J., Zhan, R. and Wu, R. 2018. Equatorial cold-water tongue in the Late Ordovician. *Geology*, **46**, 759–762, https://doi.org/10.1130/g45302.1

Joachimski, M.M. and Buggisch, W. 2002. Conodont apatite $\delta^{18}O$ signatures indicate climatic cooling as a trigger of the Late Devonian mass extinction. *Geology*, **30**, 711–714, https://doi.org/10.1130/0091-7613(2002)030<0711:CAOSIC>2.0.CO;2

Joachimski, M.M. and Lambert, L.L. 2015. Salinity contrast in the US Midcontinent Sea during Pennsylvanian glacio-eustatic highstands: evidence from conodont apatite $\delta^{18}O$. *Palaeogeography, Palaeoclimatology, Palaeoecology*, **433**, 71–80, https://doi.org/10.1016/j.palaeo.2015.05.014

Joachimski, M.M., von Bitter, P.H. and Buggisch, W. 2006. Constraints on Pennsylvanian glacioeustatic sea-level changes using oxygen isotopes of conodont apatite. *Geology*, **34**, 277–280, https://doi.org/10.1130/g22198.1

Joachimski, M.M., Breisig, S. *et al*. 2009. Devonian climate and reef evolution: insights from oxygen isotopes in apatite. *Earth and Planetary Science Letters*, **284**, 599–609, https://doi.org/10.1016/j.epsl.2009.05.028

John, E.H., Cliff, R. and Wignall, P.B. 2008. A positive trend in seawater $^{87}Sr/^{86}Sr$ values over the Early–Middle Frasnian boundary (Late Devonian) recorded in well-preserved conodont elements from the Holy Cross Mountains, Poland. *Palaeogeography, Palaeoclimatology, Palaeoecology*, **269**, 166–175, https://doi.org/10.1016/j.palaeo.2008.04.031

Katz, D.A., Buoniconti, M.R., Montañez, I.P., Swart, P.K., Eberli, G.P. and Smith, L.B. 2007. Timing and local perturbations to the carbon pool in the lower Mississippian Madison Limestone, Montana and Wyoming. *Palaeogeography, Palaeoclimatology, Palaeoecology*, **256**, 231–253, https://doi.org/10.1016/j.palaeo.2007.02.048

Korte, C. and Ullmann, C.V. 2018. Permian strontium isotope stratigraphy. *Geological Society, London, Special Publications*, **450**, 105–118, https://doi.org/10.1144/SP450.5

Lai, X.L., Wignall, P.B. and Zhang, K.X. 2001. Palaeoecology of the conodonts *Hindeodus* and *Clarkina* during the Permian–Triassic transitional period. *Palaeogeography Palaeoclimatology Palaeoecology*, **171**, 63–72, https://doi.org/10.1016/S0031-0182(01)00269-3

Li, D., Zhang, X. *et al*. 2018. Evidence of a large $\delta^{13}C_{carb}$ and $\delta^{13}C_{org}$ depth gradient for deep-water anoxia during

the late Cambrian SPICE event. *Geology*, **46**, 631–634, https://doi.org/10.1130/g40231.1

Liu, C., Jarochowska, E., Du, Y., Vachard, D. and Munnecke, A. 2015. Microfacies and carbon isotope records of Mississippian carbonates from the isolated Bama Platform of Youjiang Basin, South China: possible responses to climate-driven upwelling. *Palaeogeography, Palaeoclimatology, Palaeoecology*, **438**, 96–112, https://doi.org/10.1016/j.palaeo.2015.07.048

Liu, C., Jarochowska, E., Du, Y., Vachard, D. and Munnecke, A. 2017. Stratigraphical and $\delta^{13}C$ records of Permo-Carboniferous platform carbonates, South China: responses to late Paleozoic icehouse climate and icehouse–greenhouse transition. *Palaeogeography, Palaeoclimatology, Palaeoecology*, **474**, 113–129, https://doi.org/10.1016/j.palaeo.2016.07.038

Lowenstam, H.A. 1961. Mineralogy, O^{18}/O^{16} ratios, and strontium and magnesium contents of recent and fossil brachiopods and their bearing on the history of the oceans. *The Journal of Geology*, **69**, 241–260, https://doi.org/10.1086/626740

Maharjan, D., Jiang, G., Peng, Y. and Nicholl, M.J. 2018*a*. Sulfur isotope change across the Early Mississippian K–O (Kinderhookian–Osagean) $\delta^{13}C$ excursion. *Earth and Planetary Science Letters*, **494**, 202–215, https://doi.org/10.1016/j.epsl.2018.04.043

Maharjan, D., Jiang, G., Peng, Y. and Henry, R.A. 2018*b*. Paired carbonate-organic carbon and nitrogen isotope variations in Lower Mississippian strata of the southern Great Basin, western United States. *Palaeogeography, Palaeoclimatology, Palaeoecology*, **490**, 462–472, https://doi.org/10.1016/j.palaeo.2017.11.026

McArthur, J.M., Howarth, R.J. and Shields, G.A. 2012. Strontium isotope stratigraphy. *In*: Gradstein, F., Ogg, J., Ogg, G. and Schmitz, M. (eds) *The Geologic Time Scale 2012*. Elsevier, 127–144.

Mii, H.-S., Grossman, E.L. and Yancey, T.E. 1999. Carboniferous isotope stratigraphies of North America: Implications for Carboniferous paleoceanography and Mississippian glaciation. *Geological Society of America Bulletin*, **111**, 960–973.

Mii, H.-S., Grossman, E.L., Yancey, T.E., Chuvashov, B. and Egorov, A. 2001. Isotopic records of brachiopod shells from the Russian Platform – evidence for the onset of mid-Carboniferous glaciation. *Chemical Geology*, **175**, 133–147, https://doi.org/10.1016/S0009-2541(00)00366-1

Montañez, I.P. and Poulsen, C.J. 2013. The Late Paleozoic Ice Age: an evolving paradigm. *Annual Review of Earth and Planetary Sciences*, **41**, 629–656, https://doi.org/10.1146/annurev.earth.031208.100118

Montañez, I.P., Banner, J.L., Osleger, D.A., Borg, L.E. and Bosserman, P.J. 1996. Integrated Sr isotope variations and sea-level history of Middle to Upper Cambrian platform carbonates: implications for the evolution of Cambrian seawater $^{87}Sr/^{86}Sr$. *Geology*, **24**, 917–920, https://doi.org/10.1130/0091-7613(1996)024<0917:isivas>2.3.co;2

Montañez, I.P., Osleger, D.J. *et al*. 2018. Carboniferous climate teleconnections archived in coupled bioapatite $\delta^{18}O_{PO4}$ and $^{87}Sr/^{86}Sr$ records from the epicontinental Donets Basin, Ukraine. *Earth and Planetary Science Letters*, **492**, 89–101, https://doi.org/10.1016/j.epsl.2018.03.051

Orchard, M.J. 1996. Conodont fauna from the Permian–Triassic boundary: observations and reservations. *Permophiles*, **28**, 29–35.

Palmer, M.R. and Edmond, J.M. 1989. The strontium isotope budget of the modern ocean. *Earth and Planetary Science Letters*, **92**, 11–26, https://doi.org/10.1016/0012-821X(89)90017-4

Panchuk, K.M., Holmden, C. and Kump, L.R. 2005. Sensitivity of the epeiric sea carbon isotope record to local-scale carbon cycle processes: tales from the Mohawkian Sea. *Palaeogeography, Palaeoclimatology, Palaeoecology*, **228**, 320–337, https://doi.org/10.1016/j.palaeo.2005.06.019

Patterson, W.P. and Walter, L.M. 1994. Depletion of ^{13}C in seawater CO_2 on modern carbonate platforms: significance for the carbon isotopic record of carbonates. *Geology*, **22**, 885–888, https://doi.org/10.1130/0091-7613(1994)022<0885:DOCISC>2.3.CO;2

Popp, B.N., Anderson, T.F. and Sandberg, P.A. 1986. Brachiopods as indicators of original isotopic compositions in some Paleozoic limestones. *Geological Society of America Bulletin*, **97**, 1262–1269, https://doi.org/10.1130/0016-7606(1986)97<1262:BAIOOI>2.0.CO;2

Prokoph, A., Shields, G.A. and Veizer, J. 2008. Compilation and time-series analysis of a marine carbonate δ18O, δ13C, $^{87}Sr/^{86}Sr$ and δ34S database through Earth history. *Earth-Science Reviews*, **87**, 113–133, https://doi.org/10.1016/j.earscirev.2007.12.003

Pucéat, E., Reynard, B. and Lécuyer, C. 2004. Can crystallinity be used to determine the degree of chemical alteration of biogenic apatites? *Chemical Geology*, **205**, 83–97, https://doi.org/10.1016/j.chemgeo.2003.12.014

Qi, Y., Barrick, J.E., Hogancamp, N.J., Chen, J., Hu, K., Wang, Q. and Wang, X. 2020. Conodont faunas across the Kasimovian–Gzhelian boundary (Late Pennsylvanian) in South China and implications for the selection of the stratotype for the base of the global Gzhelian stage. *Papers in Palaeontology*, **6**, 439–484, https://doi.org/10.1002/spp2.1301.

Qie, W., Zhang, X., Du, Y. and Zhang, Y. 2011. Lower Carboniferous carbon isotope stratigraphy in South China: implications for the Late Paleozoic glaciation. *Science China Earth Sciences*, **54**, 84–92, https://doi.org/10.1007/s11430-010-4062-4

Qie, W., Wang, X.-D. *et al*. 2016. Latest Devonian to earliest Carboniferous conodont and carbon isotope stratigraphy of a shallow-water sequence in South China. *Geological Journal*, **51**, 915–935, https://doi.org/10.1002/gj.2710

Richey, J.D., Montañez, I.P., Godderis, Y., Looy, C.V., Griffis, N.P. and DiMichele, W.A. 2020. Influence of temporally varying weatherability on CO_2 – climate coupling and ecosystem change in the late Paleozoic. *Climates of the Past*, **16**, 1759–1775, https://doi.org/10.5194/cp-16-1759-2020.

Roark, A., Flake, R. *et al*. 2017. Brachiopod geochemical records from across the Carboniferous seas of North America: evidence for salinity gradients, stratification, and circulation patterns. *Palaeogeography, Palaeoclimatology, Palaeoecology*, **485**, 136–153, https://doi.org/10.1016/j.palaeo.2017.06.009

Rollion-Bard, C., Saulnier, S., Vigier, N., Schumacher, A., Chaussidon, M. and Lécuyer, C. 2016. Variability in magnesium, carbon and oxygen isotope compositions

of brachiopod shells: implications for paleoceanographic studies. *Chemical Geology*, **423**, 49–60, https://doi.org/10.1016/j.chemgeo.2016.01.007

Rollion-Bard, C., Garcia, S.M., Burckel, P., Angiolini, L., Jurikova, H., Tomašových, A. and Henkel, D. 2019. Assessing the biomineralization processes in the shell layers of modern brachiopods from oxygen isotopic composition and elemental ratios: implications for their use as paleoenvironmental proxies. *Chemical Geology*, **524**, 49–66, https://doi.org/10.1016/j.chemgeo.2019.05.031

Rosenau, N.A., Tabor, N.J. and Herrmann, A. 2014. Assessing the paleoenvironmental significance of Middle-Late Pennsylvanian conodont apatite $\delta^{18}O$ values in the Illinois basin. *Palaios*, **29**, 250–265, https://doi.org/10.2110/palo.2013.112

Ruppel, S.C., James, E.W., Barrick, J.E., Nowlan, G. and Uyeno, T.T. 1996. High-resolution $^{87}Sr/^{86}Sr$ chemostratigraphy of the Silurian: implications for event correlation and strontium flux. *Geology*, **24**, 831–834, https://doi.org/10.1130/0091-7613(1996)024<0831:HRSSCO>2.3.CO;2

Saltzman, M. 2002. Carbon and oxygen isotope stratigraphy of the Lower Mississippian (Kinderhookian–lower Osagean), western United States: implications for seawater chemistry and glaciation. *Geological Society of America Bulletin*, **114**, 96–108, https://doi.org/10.1130/0016-7606(2002)114<0096:CAOISO>2.0.CO;2

Saltzman, M.R. 2003*a*. Organic carbon burial and phosphogenesis in the Antler Foreland Basin: an out-of-phase relationship during the lower Mississippian. *Journal of Sedimentary Research*, **73**, 844–855, https://doi.org/10.1306/032403730844

Saltzman, M.R. 2003*b*. Late Paleozoic ice age: oceanic gateway or pCO_2? *Geology*, **31**, 151–154, https://doi.org/10.1130/0091-7613(2003)031<0151:lpiaog>2.0.co;2

Saltzman, M.R. 2005. Phosphorus, nitrogen, and the redox evolution of the Paleozoic oceans. *Geology*, **33**, 573, https://doi.org/10.1130/g21535.1

Saltzman, M.R. and Thomas, E. 2012. Carbon isotope stratigraphy. *In*: Gradstein, F., Ogg, J., Ogg, G. and Schmitz, M. (eds) *The Geologic Time Scale 2012*. Elsevier, 207–232.

Saltzman, M.R., Ripperdan, R.L. *et al*. 2000. A global carbon isotope excursion (SPICE) during the Late Cambrian: relation to trilobite extinctions, organic-matter burial and sea level. *Palaeogeography, Palaeoclimatology, Palaeoecology*, **162**, 211–223, https://doi.org/10.1016/s0031-0182(00)00128-0

Saltzman, M.R., Groessens, E. and Zhuravlev, A.V. 2004*a*. Carbon cycle models based on extreme changes in $\delta^{13}C$: an example from the lower Mississippian. *Palaeogeography, Palaeoclimatology, Palaeoecology*, **213**, 359–377, https://doi.org/10.1016/j.palaeo.2004.07.019

Saltzman, M.R., Cowan, C.A., Runkel, A.C., Runnegar, B., Stewart, M.C. and Palmer, A.R. 2004*b*. The Late Cambrian SPICE ($\delta^{13}C$) event and the Sauk II–SAUK III regression: new evidence from Laurentian Basins in Utah, Iowa, and Newfoundland. *Journal of Sedimentary Research*, **74**, 366–377, https://doi.org/10.1306/120203740366

Saltzman, M.R., Edwards, C.T. *et al*. 2014. Calibration of a conodont apatite-based Ordovician $^{87}Sr/^{86}Sr$ curve to biostratigraphy and geochronology: implications for stratigraphic resolution. *Geological Society of America Bulletin*, **126**, 1551–1568, https://doi.org/10.1130/b31038.1

Schiffbauer, J.D., Huntley, J.W., Fike, D.A., Jeffrey, M.J., Gregg, J.M. and Shelton, K.L. 2017. Decoupling biogeochemical records, extinction, and environmental change during the Cambrian SPICE event. *Science Advances*, **3**, e1602158, https://doi.org/10.1126/sciadv.1602158

Sharma, M., Balakrishna, K., Hofmann, A.W. and Shankar, R. 2007. The transport of Osmium and Strontium isotopes through a tropical estuary. *Geochimica et Cosmochimica Acta*, **71**, 4856–4867, https://doi.org/10.1016/j.gca.2007.08.004

Sun, Y., Joachimski, M.M. *et al*. 2012. Lethally hot temperatures during the Early Triassic greenhouse. *Science*, **338**, 366–370, https://doi.org/10.1126/science.1224126

Swart, P.K. 2015. The geochemistry of carbonate diagenesis: the past, present and future. *Sedimentology*, **62**, 1233–1304, https://doi.org/10.1111/sed.12205

Swart, P.K. and Eberli, G. 2005. The nature of the $\delta^{13}C$ of periplatform sediments: implications for stratigraphy and the global carbon cycle. *Sedimentary Geology*, **175**, 115–129, https://doi.org/10.1016/j.sedgeo.2004.12.029

Tian, X., Chen, J., Yao, L., Hu, K., Qi, Y., Wang, X. and Somerville, I. 2020. Glacio-eustasy and $\delta^{13}C$ across the Mississippian–Pennsylvanian boundary in the eastern Paleo-Tethys Ocean (South China): implications for mid-Carboniferous major glaciation. *Geological Journal*, **55**, 2704–2716, https://doi.org/10.1002/gj.3551

Trotter, J.A., Willians, I.S., Barnes, C.R., Lecuyer, C. and Nicoll, R.S. 2008. Did cooling oceans trigger Ordovician biodiversification? Evidence from conodont thermometry. *Science*, **321**, 550–554, https://doi.org/10.1126/science.1155814

Veizer, J. and Hoefs, J. 1976. The nature of O^{18}/O^{16} and C^{13}/C^{12} secular trends in sedimentary carbonate rocks. *Geochimica et Cosmochimica Acta*, **40**, 1387–1395, https://doi.org/10.1016/0016-7037(76)90129-0

Veizer, J., Fritz, P. and Jones, B. 1986. Geochemistry of brachiopods: oxygen and carbon isotopic records of Paleozoic oceans. *Geochimica et Cosmochimica Acta*, **50**, 1679–1696, https://doi.org/10.1016/0016-7037(86)90130-4

Veizer, J., Ala, D. *et al*. 1999. $^{87}Sr/^{86}Sr$, $\delta^{13}C$ and $\delta^{18}O$ evolution of Phanerozoic seawater. *Chemical Geology*, **161**, 59–88, https://doi.org/10.1016/S0009-2541(99)00081-9

Wallace, Z.A. and Elrick, M. 2014. Early Mississippian orbital-scale glacio-eustasy detected from high-resolution oxygen isotopes of marine apatite (conodonts). *Journal of Sedimentary Research*, **84**, 816–824, https://doi.org/10.2110/jsr.2014.69

Wang, W.-Q., Garbelli, C. *et al*. 2020. A high-resolution Middle to Late Permian paleotemperature curve reconstructed using oxygen isotopes of well-preserved brachiopod shells. *Earth and Planetary Science Letters*, **540**, 116245, https://doi.org/10.1016/j.epsl.2020.116245

Wang, X.D., Hu, K.Y. *et al*. 2019. Carboniferous integrative stratigraphy and time scale of China. *Science China Earth Sciences*, **62**, 135–153, https://doi.org/10.1007/s11430-017-9253-7

Wang, Z., Chen, J. *et al*. 2020. Spatial variation in carbonate carbon isotopes during the Cambrian SPICE event across the eastern North China Platform. *Palaeogeography, Palaeoclimatology, Palaeoecology*, **546**, 109669, https://doi.org/10.1016/j.palaeo.2020.109669

Wenzel, B., Lécuyer, C. and Joachimski, M.M. 2000. Comparing oxygen isotope records of silurian calcite and phosphate – $\delta^{18}O$ compositions of brachiopods and conodonts. *Geochimica et Cosmochimica Acta*, **64**, 1859–1872, https://doi.org/10.1016/s0016-7037(00)00337-9

Woodard, S.C., Thomas, D.J., Grossman, E.L., Olszewski, T.D., Yancey, T.E., Miller, B.V. and Raymond, A. 2013. Radiogenic isotope composition of Carboniferous seawater from North American epicontinental seas. *Palaeogeography, Palaeoclimatology, Palaeoecology*, **370**, 51–63, https://doi.org/10.1016/j.palaeo.2012.11.018

Yamamoto, K., Asami, R. and Iryu, Y. 2010. Within-shell variations in carbon and oxygen isotope compositions of two modern brachiopods from a subtropical shelf environment off Amami-o-shima, southwestern Japan. *Geochemistry, Geophysics, Geosystems*, **11**, Q10009, https://doi.org/10.1029/2010gc003190

Yao, L., Qie, W. *et al*. 2015. The TICE event: perturbation of carbon–nitrogen cycles during the mid-Tournaisian (Early Carboniferous) greenhouse–icehouse transition. *Chemical Geology*, **401**, 1–14, https://doi.org/10.1016/j.chemgeo.2015.02.021

Zaky, A.H., Brand, U. *et al*. 2019. Strontium isotope geochemistry of modern and ancient archives: tracer of secular change in ocean chemistry. *Canadian Journal of Earth Sciences*, **56**, 245–264, https://doi.org/10.1139/cjes-2018-0085

Zazzo, A., Lécuyer, C. and Mariotti, A. 2004. Experimentally-controlled carbon and oxygen isotope exchange between bioapatites and water under inorganic and microbially-mediated conditions. *Geochimica et Cosmochimica Acta*, **68**, 1–12, https://doi.org/10.1016/s0016-7037(03)00278-3

Zhou, Y., Pogge von Strandmann, P.A.E. *et al*. 2020. Reconstructing Tonian seawater $^{87}Sr/^{86}Sr$ using calcite microspar. *Geology*, **48**, 462–467, https://doi.org/10.1130/g46756.1